Testing realistic SO(10) SUSY GUTs with proton decay and gravitational waves

Bowen Fu,[1,*] Stephen F. King,[1,†] Luca Marsili,[2,‡] Silvia Pascoli,[3,4,§] Jessica Turner,[2,‖] and Ye-Ling Zhou[5,6,¶]

[1]*School of Physics and Astronomy, University of Southampton, Southampton, SO17 1BJ, United Kingdom*
[2]*Institute for Particle Physics Phenomenology, Department of Physics, Durham University, Durham DH1 3LE, United Kingdom*
[3]*DIFA, University of Bologna, via Irnerio 46, 40126 Bologna, Italy*
[4]*INFN, Sezione di Bologna, viale Berti Pichat 6/2, 40127 Bologna, Italy*
[5]*School of Fundamental Physics and Mathematical Sciences, Hangzhou Institute for Advanced Study, UCAS, Hangzhou 310024, China*
[6]*International Centre for Theoretical Physics Asia-Pacific, Beijing/Hangzhou, China*

(Received 28 August 2023; accepted 21 February 2024; published 14 March 2024)

We present a comprehensive analysis of a supersymmetric SO(10) grand unified theory, which is broken to the Standard Model via the breaking of two intermediate symmetries. The spontaneous breaking of the first intermediate symmetry, $B-L$, leads to the generation of cosmic strings and right-handed neutrino masses and further to an observable cosmological background of gravitational waves and generation of light neutrino masses via type-I seesaw mechanism. Supersymmetry breaking manifests as sparticle masses below the $B-L$ breaking but far above the electroweak scale due to proton decay limits. This naturally pushes the $B-L$ breaking scale close to the grand unified theory scale, leading to the formation of metastable cosmic strings, which can provide a gravitational wave spectrum consistent with the recent pulsar timing arrays observation. We perform a detailed analysis of this model using two-loop renormalization group equations, including threshold corrections, to determine the symmetry-breaking scale consistent with the recent pulsar timing arrays signals such as NANOGrav 15-year data and testable by the next-generation limits on proton decay from Hyper-K and JUNO. Simultaneously, we find the regions of the model parameter space that can predict the measured quark and lepton masses and mixing, baryon asymmetry of our Universe, a viable dark matter candidate and can be tested by a combination of neutrinoless double beta decay searches and limits on the sum of neutrinos masses.

DOI: 10.1103/PhysRevD.109.055025

I. INTRODUCTION

SO(10) grand unified theories (GUTs) are widely studied, ultraviolet complete frameworks that unify three of the fundamental forces and have unique features [1–3]:

(1) Highly correlated fermion masses and mixing as quarks and leptons are arranged in a single representation in the GUT gauge space.
(2) Inclusion of a $U(1)_{B-L}$ gauge symmetry, whose spontaneous breaking gives rise to cosmic strings [4] and right-handed neutrino masses, which can generate light Majorana masses for neutrinos and a baryon asymmetry.
(3) Generically, baryon and lepton number violating operators that induce proton decay and allow to set stringent limits on the GUT breaking scale.

These features of SO(10) GUTs allow to constrain the models with present and future data from a variety of complementary approaches. Next-generation large-scale neutrino experiments, including JUNO [5], DUNE [6], and Hyper-Kamiokande [7], are expected to measure the majority of neutrino oscillation parameters at percent level precision. An additional goal of these experiments will be to constrain, or possibly even measure, the proton lifetime at an unprecedented level. Both measurements will probe the theory parameter space of SO(10) GUTs. Moreover, as discussed above, a generic feature of many GUTs is the

*B.Fu@soton.ac.uk
†king@soton.ac.uk
‡luca.marsili@durham.ac.uk
§silvia.pascoli@unibo.it
‖jessica.turner@durham.ac.uk
¶zhouyeling@ucas.ac.cn

Published by the American Physical Society under the terms of the Creative Commons Attribution 4.0 International license. Further distribution of this work must maintain attribution to the author(s) and the published article's title, journal citation, and DOI. Funded by SCOAP³.

breaking of a $U(1)$ gauge symmetry which can generate a network of cosmic strings [8]. If the string network is not completely diluted by inflation, it may be a source of stochastic gravitational wave background (SGWB) with a broad spectrum of frequency from nanohertz to kilohertz. Due to this broad spectrum, a variety of currently running and upcoming gravitational wave (GW) experiments, including those from pulsar timing arrays (PTAs), space- and ground-based laser interferometers, as well as atomic interferometers, will be able to constrain such GUTs [9–13]. Very recently, the NANOGrav collaboration with 15 years of data activity (NANOGrav15) [14–18] reported the evidence for quadrupolar correlations [19], indicating a GW origin of the signal. Similar evidences have been independently reported by EPTA [20–25], PPTA [26–28], and CPTA [29]. Based on the Bayesian analysis of NANOGrav15, it was shown that the Nambu-Goto (NG) strings do not provide a good fit to the signal [18] and sets a stringent bound on the symmetry breaking scale for stable strings. The possibility that metastable cosmic strings [30–32] or superstrings [33] may be the source of the observed SGWB remains open.

We have shown that this rapid progress in neutrino and gravitational wave measurements provides complementary probes of SO(10) GUTs [34,35], offering a unique opportunity to indirectly test very high energy scales. In Ref. [36], we carried out a detailed study of SO(10), showing that all Standard Model (SM) fermion masses and mixing parameters and the baryon asymmetry can be matched to their observed values in this model. In that work, we constructed a model with a $U(1)_{B-L}$ symmetry breaking scale around 10^{13} GeV, that is not excluded by PTAs but cannot explain the newer indications of SGWB that may originate from metastable strings.

In this paper, we continue our roadmap on the testability of SO(10) GUTs by extending the analysis to a supersymmetric (SUSY) version. As we will show, SUSY GUT can have marked differences with respect to the non-SUSY models considered already. It offers a natural framework for metastable strings consistent with the NANOGrav signal, as it favors a $U(1)_{B-L}$ breaking very close to the GUT scale. In addition to being currently one of the favored explanation to the SGWB signal recently observed by the PTA observatories, thanks to its rather broad frequency spectrum the resulting SWGB will be within the sensitivity of future GW experiments at higher frequencies. Moreover, one of the key predictions of SUSY GUTs is kaonic proton decay ($p \to K\bar{\nu}$), in addition to the other non-SUSY decay channels. In the coming years, JUNO will provide the best sensitivity to this channel and place a key constraint on SUSY GUTs.

We perform a comprehensive analysis of this model by determining each scale of symmetry breaking by solving the renormalization group equations (RGEs) and fitting our model to SM fermion masses and mixing data. We concretely demonstrate that the predictions of our model can be tested by next-generation cosmic microwave background observations, neutrinoless double beta decay, oscillation measurements, GW experiments, and searches for proton decay. Moreover, our model can predict the observed baryon asymmetry and accommodate a viable dark matter candidate.

II. MODEL FRAMEWORK

The model we present and confront with flavor, proton decay, and gravitational wave data is a SUSY SO(10) GUT, that is spontaneously broken to the SM as follows:

$$\begin{aligned} & SO(10)\times \mathrm{SUSY} \\ & \quad \mathbf{45} \downarrow \text{broken at } M_{\mathrm{GUT}} \\ & G_{\mathrm{LRSM}} \equiv SU(3)_c \times SU(2)_L \times SU(2)_R \times U(1)_{B-L} \times \mathrm{SUSY} \\ & \quad \overline{\mathbf{126}} \downarrow \text{broken at } M_{B-L} \\ & G_{\mathrm{MSSM}} \equiv SU(3)_c \times SU(2)_L \times U(1)_Y \times \mathrm{SUSY} \\ & \quad \downarrow \text{broken at } M_{\mathrm{SUSY}} \\ & G_{\mathrm{SM}} \equiv SU(3)_c \times SU(2)_L \times U(1)_Y. \end{aligned} \tag{1}$$

At scale M_{GUT}, the GUT symmetry is broken, and dimension-six operators which mediate proton decay are induced. This GUT symmetry breaking also leads to the production of monopoles which we assume are removed through a period of rapid inflation. The next breaking step occurs at M_{B-L}, where the $U(1)_{B-L}$ gauge symmetry is spontaneously broken. This leads to the production of a network of cosmic strings, that can decay gravitationally, as well as to the generation of right-handed neutrino (RHN) masses. These RHNs can decay to produce a matter-antimatter asymmetry via thermal leptogenesis [37]. In the final step, SUSY is broken at a scale M_{SUSY}, defined to be equal to the common masses of the squarks and sleptons, and dimension-five operators which mediate proton decay are induced via wino and Higgsino exchange, whose masses, $M_{\tilde{W}}$, are allowed to be below M_{SUSY}. This is typical of widely studied split SUSY scenarios [38,39]. The boldface numbers to the left of the arrows of Eq. (1) denote the representations of Higgs superfields of SO(10) required for the symmetry breaking.

In Ref. [35], we analyzed all symmetry-breaking patterns of a non-SUSY SO(10) GUT to the SM via the Pati-Salam path by solving the two-loop RGEs and assuming gauge coupling unification at M_{GUT}. We found that the majority of breaking patterns constrain $M_{B-L} \lesssim 10^{13}$ GeV with no symmetry breaking patterns attaining $M_{B-L} \gtrsim 10^{14}$ GeV. This leads to the formation of cosmic strings with a relatively small string tension which is more difficult to be tested by GW interferometers. One notable motivation to extend from non-SUSY GUTs to SUSY GUTs is that, in the SUSY version, M_{B-L} can naturally reach

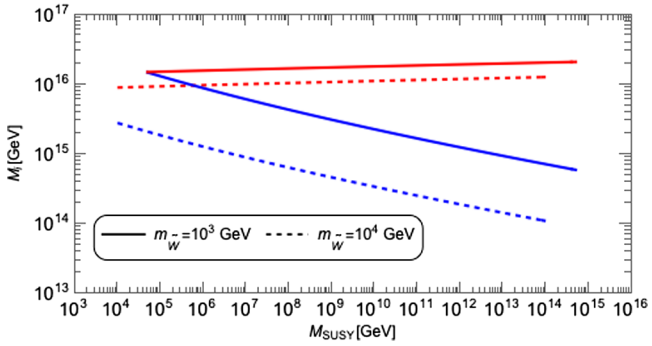

FIG. 1. The GUT scale, $M_{\rm GUT}$ (red), and $U(1)_{B-L}$ breaking scale, M_{B-L} (blue), as a function of the SUSY breaking scale $M_{\rm SUSY}$, defined as the common squark and slepton mass scale. The solid and dashed lines show the effect on the RGEs solutions for various wino masses, assumed to be below $M_{\rm SUSY}$. For an observable GW signal, the inflationary scale must lie between the red and blue lines.

10^{14}–10^{15} GeV, which leads to the formation of very heavy metastable strings that can accommodate the GW signal detected by the PTAs. To determine the $B-L$ breaking scale in the SUSY version, we follow the same procedure as our previous work Ref. [35], by solving the two-loop RGEs, including threshold effects from gauginos and Higgsino masses, which may be a few orders of magnitude lower than $M_{\rm SUSY}$. The β coefficients at each intermediate scale are listed in Appendix A. From our RGE analysis, we find that the lower the scale of SUSY breaking, the higher the $U(1)_{B-L}$ symmetry breaking scale as shown in Fig. 1. As the wino mass increases, the $B-L$ scale is suppressed while the GUT scale remains roughly the same, enlarging the hierarchy between the two scales, that leads to a stable network of strings. We use the RGE solutions as input for determining the proton decay rate and gravitational wave signal. In the following, we discuss the testability of this model.

A. Fermion masses and mixing angles

At the GUT scale, the Yukawa superpotential is given by

$$W_{\rm Y} = Y^*_{\mathbf{10}}\mathbf{16}\cdot\mathbf{16}\cdot\mathbf{10} + Y^*_{\overline{\mathbf{126}}}\mathbf{16}\cdot\mathbf{16}\cdot\overline{\mathbf{126}} + Y^*_{\mathbf{120}}\mathbf{16}\cdot\mathbf{16}\cdot\mathbf{120} + \text{H.c.}, \quad (2)$$

where the asterisk denotes complex conjugation, **16** is the SO(10) matter multiplet and **10**, $\overline{\mathbf{126}}$ and **120** are the Higgs superfields. See Appendix B for more details. In flavor space, the Yukawa matrices are 3×3 with $Y_{\mathbf{10}}$ and $Y_{\overline{\mathbf{126}}}$ complex, symmetric and $Y_{\mathbf{120}}$ real, antisymmetric. We treat the quark masses and Cabibbo–Kobayashi–Maskawa (CKM) mixing parameters [40,41] as inputs and hence this model has seven free parameters which we vary to predict eight observables in the lepton sector.

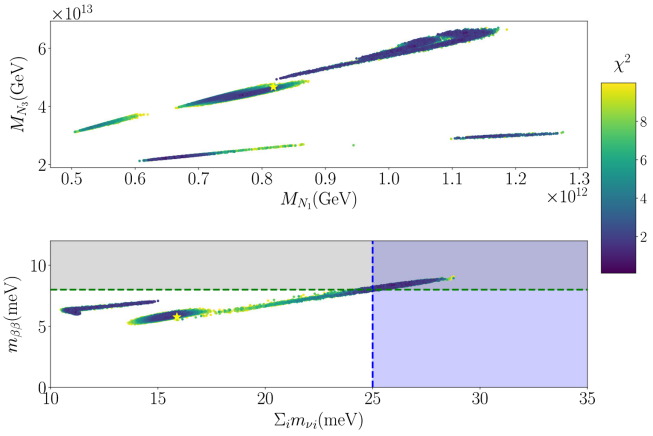

FIG. 2. All colored points show regions of the parameter space that fit the neutrino sector with $\chi^2 < 10$. The yellow star shows a benchmark point in the scan with $\eta_B \sim 6.2\times 10^{-10}$. All the points in the scan predict $-10 \lesssim \log_{10}(\eta_B) \lesssim -8$. In the upper plot, we see that the heaviest right-handed neutrino mass is predicted to be $M_{N_3} \sim 10^{13}$ GeV, with the lightest right-handed neutrino mass M_{N_1} an order of magnitude less, and the mass hierarchy is mild, with the lightest right-handed neutrino mass M_{N_1} an order of magnitude less. In the lower plot, we show the effective neutrino mass ($m_{\beta\beta}$) predicted from our model as a function of the sum of neutrino masses. The grey regions shows the reach of the next generation $\nu 0\beta\beta$ experiments and the blue region shows the sensitivity for EUCLID [52,53].

We perform the procedure using MultiNest [42] to minimize the χ^2 statistical measure as detailed in Appendix C.

B. Leptogenesis and $0\nu\beta\beta$ decay

For the points in the model parameter space scan which fits the flavor data at high statistical significance, there is a prediction for the Yukawa matrix, Y_ν, which couples the RHNs to the leptonic and Higgs doublets and the mass spectrum for the RHNs where the latter is shown in the upper panel of Fig. 2. The heaviest right-handed neutrino mass is constrained at around $M_{N_3} \sim 10^{13}$ GeV and we observed that there is a mild mass hierarchy predicted. We can calculate the baryon asymmetry generated from the decays of these RHNs using ULYSSES [43,44] to solve the density matrix equations. All points of the scan that fit the flavor data allow for viable leptogenesis with a baryon asymmetry of the same order or larger than the observed value [45]. We found that the model parameter space highly favors normally ordered neutrino masses, with the lightest neutrino mass in the range $5 \lesssim m_{\nu_1}(\text{meV}) \lesssim 15$. In the lower panel of Fig. 2, we show the predictions of our scan for the effective Majorana mass ($m_{\beta\beta}$) as a function of the sum of neutrino masses ($\sum_i m_{\nu_i}$). Both observables are testable by the next generation of $\nu 0\beta\beta$ [46–50] and cosmic microwave background experiments [51–53] with their sensitivities shown in gray and blue, respectively. We note that all the points shown fit the flavor data well

($\chi^2 \lesssim 10$), and our benchmark point (indicated by the associated yellow star in Fig. 2 see Appendix C 2 for the Yukawa matrices) is consistent with the flavor data ($\chi^2 \lesssim 3$) and provides a prediction of the baryon-to-photon ratio $\eta_B \sim 6.2 \times 10^{-10}$.

C. Proton decay

The proton decay bound on the GUT scale can be translated to the restriction on the SUSY breaking scale and wino mass from the solutions of the RGEs (see Fig. 1) and the assumption of gauge coupling unification. Increasing $m_{\tilde{W}}$ suppresses $M_{\rm GUT}$, and therefore increases the proton decay rate to a level which can be tested in Hyper-K, as later summarized in Fig. 5. Such low mass sparticles may be within reach at the FCC [54], offering another avenue to test the model. As the GUT we study is supersymmetric, additional contributions to proton decay from the color-triplet Higgs superfields can mediate the baryon-antilepton transition. The consequence is that some decay channels, such as $p \to K^+\bar{\nu}$, are enhanced. Although this channel is less well experimentally constrained, $\tau_{K\bar{\nu}} \gtrsim 5.9 \times 10^{33}$ years in Super-K [55], the SUSY GUT provides $\tau_{K\bar{\nu}} \propto M_{\rm GUT}^2 M_{\rm SUSY}^2$, and thus this channel can lead to stronger constraints on the SUSY GUT. Since we consider split SUSY spectrum, there is an additional enhancement to the partial lifetime by a factor $M_{\rm SUSY}^2/m_{\tilde{W}}^2$ in the case $m_{\tilde{W}} \ll M_{\rm SUSY}$. Moreover, as this channel originates from the Yukawa superpotential in Eq. (2), the partial lifetime is determined by the Yukawa coupling matrices, which are almost entirely fixed, up to overall order-one factors, by our fit to the fermion flavor data. Further details of the proton lifetime calculations are provided in Appendix D. We will discuss how the pionic and kaonic decay channels can constrain the GUT model parameter space and the nontrivial interplay with the GW predictions in the discussion section.

D. Dark matter

If R-parity is conserved after SUSY breaking, the lightest SUSY particle (LSP) would be stable and thus can be a dark matter candidate if it is a neutralino [56,57]. Due to the observed relic abundance, an upper limit on the mass of LSP can be obtained to avoid overabundance. Generally, the lightest neutralino can be the mixture of wino, bino, and Higgsino. The maximal dark matter mass can be as high as 10 TeV with resonant heavy Higgs annihilation or enhancement in annihilation rate through next to LSP [58]. On the other hand, a pure bino LSP or bino-dominated LSP commonly leads to an overabundance unless (co)annihilation processes further reduce the relic density. The upper limit of pure wino dark matter mass is around 3 TeV [59], and for pure Higgsino the limit is around 1 TeV [38] which can account for the correct dark matter relic density.

E. Gravitational waves

When a $U(1)$ symmetry is broken at a certain scale M_{B-L}, a cosmic strings network is generated. The long strings in the network can intersect to form loops that oscillate and emit energy via gravitational radiation. Such radiation is not coherent and can be seen as a stochastic background of gravitational waves. Importantly, this background can, in principle, be observed by currently running and future GW experiments.

We begin with the Nambu-Goto string approximation, where the string is infinitely thin with no couplings to particles [60], and the amplitude of the relic GW density parameter is

$$\Omega_{\rm GW}(f) = \frac{1}{\rho_c}\frac{d\rho_{\rm GW}}{d\log f}, \tag{3}$$

where ρ_c is the critical energy density of the Universe and $\rho_{\rm GW}$ depends on a single parameter, $G\mu$ where $G = M_{\rm pl}^{-2}$ is Newton's constant and μ is the string tension. For strings generated from the gauge symmetry $G_{\rm int} = SU(3)_c \times SU(2)_L \times SU(2)_R \times U(1)_{B-L}$, $G\mu$ is approximately given by [61]

$$G\mu \simeq \frac{1}{2(\alpha_{2R}(M_{B-L}) + \alpha_{1X}(M_{B-L}))}\frac{M_{B-L}^2}{M_{\rm pl}^2}. \tag{4}$$

In the case that M_{B-L} is not far away from $M_{\rm GUT}$, the deviation of $\alpha_{2R}(M_{B-L})$ and $\alpha_{1X}(M_{B-L})$ from $\alpha_{\rm GUT}(M_{\rm GUT})$ due to RG running is small. So we can approximate

$$G\mu \simeq \frac{1}{4\alpha_{\rm GUT}(M_{\rm GUT})}\frac{M_{B-L}^2}{M_{\rm pl}^2}. \tag{5}$$

Moreover, hence we can relate the string tension parameter to the intermediate scale M_{B-L}.

As the model we consider has $U(1)$ breaking energy scale close to the GUT symmetry breaking (which generates monopoles), the cosmic strings network can decay via monopole-antimonopole nucleation as studied in Refs. [11,62,63]. After the stage of string formation, the cosmic strings network and the consequent loops start to decay producing monopoles-antimonopoles pairs. The exponential suppression of the loop number density is characterized by the decay width per unit length Γ_d,

$$\Gamma_d = \frac{\mu}{2\pi}e^{-\pi\kappa}, \qquad \kappa = \frac{m^2}{\mu}, \tag{6}$$

for strings and the consequent loops, where $m = \frac{M_V}{\alpha} f_{\rm m}$ the monopole mass, and $f_{\rm m}$ is an undetermined factor depending on the model's detail usually assumed of order one [64]. In practice, it translates into a cutoff in the low-frequency

spectrum of the gravitational waves background which avoids the region tested by pulsar time arrays and provides the appropriate tilt in the spectrum observed by the PTA experiments. These signals can be tested by high-energy gravitational waves experiments such as the Einstein Telescope and, at high energies, by LIGO-Virgo-KAGRA (LVK) collaboration.

Although the stable cosmic strings are disfavored, the source of the signal detected by the PTAs [14,18,20,28,29] may be a network of metastable cosmic strings, which occurs when the string network decays to monopole-antimonopole pairs [65–69]. The hierarchy between the GUT scale and the string formation scale can be parametrized by

$$\sqrt{\kappa} \simeq \alpha_{\mathrm{GUT}}^{-1/2} \frac{M_{\mathrm{GUT}}}{M_{B-L}}, \tag{7}$$

where an order-one coefficient is ignored. The smaller κ, the closer the GUT and string scales and the more efficient the annihilation of the string network. As we have shown, this SUSY SO(10) GUT prefers a small hierarchy between M_{GUT} and M_{B-L}, which naturally leads to a prediction of metastable cosmic strings. Metastable strings have been suggested as a possible explanation of the PTA observations that favor $\sqrt{\kappa} \approx 8$. We can use the PTA observations as one of the strongest constraints for a stable network of cosmic strings requiring that $G\mu < 2 \times 10^{-10}$ [16] when $\sqrt{\kappa} \gg 9$, which corresponds to $M_{B-L} \lesssim 6 \times 10^{13}$ GeV due to Eq. (5).

By assuming gauge unification, we can directly connect the intermediate scale of the GUT symmetry breaking with the SUSY breaking scale, which we assume to be of the same order of magnitude as the sfermions masses. Therefore, we can constrain the SUSY breaking scale using gravitational waves. It is worth noticing that the link between the SUSY breaking scale and M_{B-L} depends on the mass of the gauginos, which, as we can see in Fig. 1, heavily affects the running of the gauge coupling.

F. Results and discussion

Here, we consider the various GUT observables and their interplay and focus on three benchmark points, representative of the three key behaviors of the model:

- BP1 This has a high SUSY-breaking scale ($M_{\mathrm{SUSY}} \sim 10^9$ GeV) as well as wino masses, leading to a $B-L$ breaking scale which is lower than BP2 and BP3. The model exhibits characteristics very similar to the non-SUSY SO(10) GUT.
- BP2 The SUSY and wino mass scales are still quite high but lower than BP1, and a prediction for proton decay via the SUSY channel $p \to K\nu$ can be achieved close to current bounds. Therefore, this case could be differentiated from non-SUSY SO(10).
- BP3 This is the most characteristic case for this model. Thanks to the low wino mass and relatively low SUSY mass scale, the $B-L$ breaking scale is very close to M_{GUT} leading to the possible generation of metastable strings and a viable explanation of NANOGrav15. A sizable prediction for the SUSY proton decay channel also emerges.

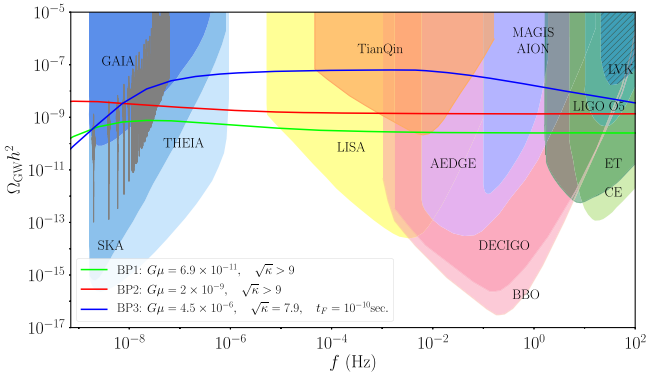

FIG. 3. GW spectra of the benchmark points. The model naturally accommodates a signal generated by a partially inflated metastable network (BP3, blue), which supports NANOGrav15. BP1 (BP2) shown in green (red) predicts stable strings which is consistent (inconsistent) with the PTA observations.

In Fig. 3, we study in detail the GW predictions in the three cases, confronting them with NANOGrav15 and the LVK bounds [70] on the spectrum at the high-frequency band. For BP1, the green curve shows the GW spectrum from stable strings, consistent with all constraints, including the upper bound set by PTA. We note that this benchmark does not provide an explanation of the PTA observation. For BP2, the red curve shows a GW spectrum from stable strings with a larger $G\mu$ value, that is inconsistent with the PTA observations, showing the importance of GW observations in constraining the model (this assumes a sufficiently high inflationary scale). Finally, for BP3, the blue curve shows the GW spectrum from metastable strings diluted by the inflation in the high-frequency band, which fits NANOGrav15 very well and is testable with future GW observations. It is important to note that since the generation of a metastable string network requires $M_{B-L} \sim M_{\mathrm{GUT}}$, without any other assumptions, this model tends to favor a signal that would be excluded by the current observations from LVK [70]. Therefore, to provide an explanation of the PTA observations, we require the cosmic string network to be partially diluted by inflation [31,71], thereby suppressing the signal in the higher frequency regime. Since M_{B-L}, M_{GUT}, and inflation are at approximately the same scale in such a scenario, it is plausible to have the cosmic string network generated towards the end of inflation and, therefore, are slightly inflated away with a typical $1/f$ suppression in the region in the high-frequency regime, as shown in Fig. 3, for a typical time $t_F \sim 10^{-10}$ s.

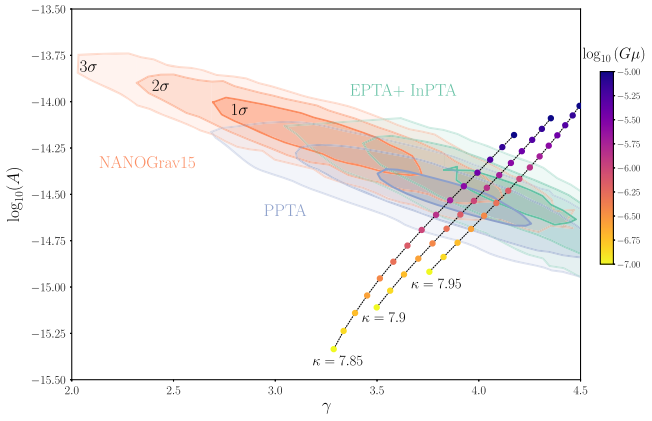

FIG. 4. Comparison between SGWB produced by a metastable network of cosmic strings with $G\mu$ from 10^{-7} to 10^{-5} and three different values of κ, and the 1σ, 2σ, 3σ regions of the signal detected by NANOGRAV [14], EPTA [20], and PPTA [28].

Assuming a power-law spectrum of the characteristic GW strain, the GW energy density spectrum can be parametrized by two parameters: the amplitude parameter, A, and power parameter, γ. Indeed, the characteristic strain of the signal detected by pulsar time arrays can be parametrized as

$$h_c(f) = A\left(\frac{f}{f_{\rm yr}}\right)^{\gamma}, \tag{8}$$

and the GW energy density spectrum, in the nHz region, is given by [72]

$$\Omega(f) = \Omega_{\rm yr}\left(\frac{f}{f_{\rm yr}}\right)^{5-\gamma}, \tag{9}$$

where $\Omega_{\rm yr} = \frac{2\pi^2}{3H_0^2}A^2 f_{\rm yr}^2$. We perform the fit in the interval 2–59 nHz following the procedure of Refs. [36,72], and the results are shown in Fig. 4, where the value of A and γ favored by observation is compared with the prediction of the metastable cosmic string network. The reference frequency of the PTA results is chosen to be 1 $\rm yr^{-1}$. We found that the signal produced by a metastable network of cosmic strings is compatible with the EPTA and PPTA in the 1σ range and with NANOGrav in the 2σ region. From Fig. 4 we note that the predicted signal is very sensitive to the value of κ. Further, the values of $G\mu$ consistent with the observations from the pulsar time array observatories get higher as κ becomes smaller. For the values of κ we have shown, $\kappa = 7.85, 7.9, 7.95$, the values of $G\mu$ for which the predicted signal is within the 2σ region, are between 10^{-5} and 10^{-7}, depending on κ, and they are consistent to the scenario in which $M_{B-L} \simeq M_{\rm GUT}$.

The benchmark points can be located also in Fig. 5, which presents the testability of this model in the $M_{\rm SUSY} - m_{\tilde{W}}$ plane. The hatched region on the top-left indicates $(m_{\tilde{W}} > M_{\rm SUSY})$ is disfavored in most SUSY scenarios.

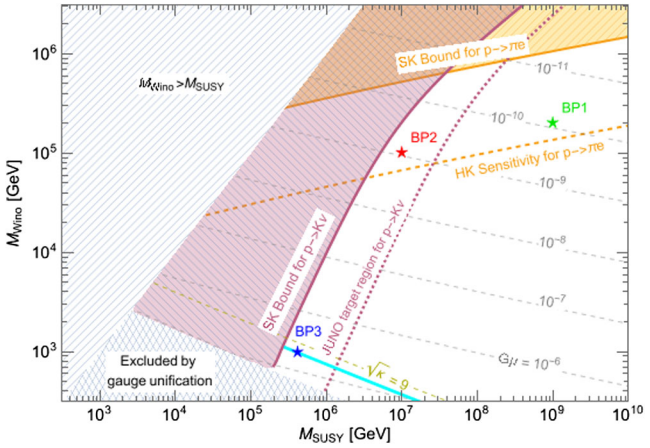

FIG. 5. Constraints and sensitivities on proton decay in the $M_{\rm SUSY} - M_{\rm Wino}$ plane, (where $M_{\rm SUSY}$ is defined as the squark and slepton mass scale). The orange lines show the constraint of Super-K (solid) and sensitivity of Hyper-K (dashed) on the $p \to \pi^0 e^+$ channel proton decay [7]. Super-K excludes the parameter space to the left of the purple solid line due to strong $p \to K^+\bar{\nu}$ channel decay. To the left of the purple dashed line, the model can predict a proton lifetime that is within the sensitivity of JUNO [5]. The narrow cyan region shows where the NANOGrav result can be explained at 95% confidence [16].

Gauge unification excludes the grid region on the bottom-left and the purple and orange solid lines are excluded by the current bounds on $\tau_{K^+\bar{\nu}}$ and $\tau_{\pi^0 e^+}$ from SUSY and non-SUSY contributions, respectively. The orange dashed line indicates the sensitivity of Hyper-K to $\pi^0 e^+$ channel decay, while the purple dashed line shows the potential target region of JUNO on $K^+\bar{\nu}$ channel decay. A summary of the predictions of the model for different benchmark points is given in Table I. BP1 has a phenomenology similar to non-SUSY SO(10) models [36]. BP2 predicts proton decay rates that Hyper-K and JUNO can probe, although it has a string tension too high to be compatible with PTA observations. The region of the parameter space that predicts metastable strings that can explain the PTA observations, such as BP3, is in the region $G\mu \gtrsim 10^{-6}$ with $\sqrt{\kappa} \sim 8$ and can predict proton decay rates in the kaon channel at reach at JUNO, but interestingly, not at Hyper-K. Moreover, we notice that this region requires wino masses that are at reach at present or future colliders, Refs. [54,73–75], with lower masses the lower the proton decay rate. Interestingly, most

TABLE I. Complementary predictions of benchmark point (BP) in the next-generation proton decay measurements and NANOGrav15.

	Hyper-K sensitivity	JUNO target	NANOGrav15
BP1	Testable	No signal	Consistent
BP2	Testable	Targeted	Inconsistent
BP3	No signal	Targeted	Support

of the parameter space that predicts proton decay rates too small to be observed by Hyper-K or JUNO is inconsistent with PTA observations.

In the nonsupersymmetric SO(10) unification, it is also possible to obtain gauge unification, predict fermion masses and mixing, and the dark matter [76]. However, to achieve successful gauge unification and leptogenesis in the non-SUSY SO(10) framework with a simple mass spectrum, the intermediate scale, which generates right-handed neutrinos masses and cosmic strings, is at least an order of magnitude smaller than the GUT scale [35,36]. In that case, intermediate $U(1)$ symmetry breaking can only lead to stable cosmic strings and thus the resulting gravitational wave cannot provide an explanation of the spectrum observed by PTAs. On the contrary, the intermediate $U(1)$ symmetry-breaking scale can be naturally close to the GUT scale in SUSY SO(10) GUTs, which leads to the prediction of a metastable cosmic string network that can explain the PTA observations. Moreover, the proton decay predicted by SUSY GUTs is in general faster than that predicted by non-SUSY GUTs due to the additional kaon channel. As a result, the SUSY GUTs is more testable than the non-SUSY ones. As shown in Fig. 5, the current bound on kaon channel proton decay rules out the possibility of low scale SUSY, which explains the absence of superpartners at LHC. Apart from the phenomenological perspectives, the hierarchy problem also motivates SUSY theoretically, further making SUSY SO(10) an attractive candidate for unification.

III. SUMMARY

We have presented a SUSY SO(10) GUT which can successfully predict fermion masses and mixing angles, leptogenesis, dark matter and can be tested via proton decay and GW signatures at next-generation experiments. The $B-L$ breaking scale correlates with the SUSY breaking scale (the squark and slepton mass scale) via the gauge unification. The natural proximity of the GUT breaking scale and the $B-L$ breaking scale leads to metastable cosmic strings decaying to monopole-antimonopole pairs, and we find that the GW signal from metastable strings can be consistent with the NANOGrav 15-year data. Considering a split-SUSY scenario we found that proton decay measurements and PTA observations cover complementary regions of the parameter space. An eventual observation of proton decay from both the pion and kaon channels is not consistent with the current PTA observations. Exploiting this complementarity, we can, therefore, test the majority of the parameter space. Regarding the interpretation of the observed GW signal as generated by a metastable cosmic string network, we found that it is consistent with our model if the signal is partially inflated away, and that it is possible to fully test this possibility with the next-generation GW observatories and JUNO and/or collider searches.

ACKNOWLEDGMENTS

We want to thank Stefan Antusch and Shaikh Saad for the helpful discussion. This work was partially supported by Chinese Scholarship Council (CSC) Grant No. 201809210011 under agreements [2018]3101 and [2019]536, European Union's Horizon 2020 Research, Innovation Programme under Marie Sklodowska-Curie grant agreement HIDDeN European ITN project (Grant No. H2020-MSCA-ITN-2019//860881-HIDDeN), National Natural Science Foundation of China (NSFC) under Grants No. 12205064, Zhejiang Provincial Natural Science Foundation of China under Grant No. LDQ24A050002, STFC Consolidated Grant No. ST/T000775/1. This work used the DiRAC@Durham facility managed by the Institute for Computational Cosmology on behalf of the STFC DiRAC HPC Facility [77], which is part of the National e-Infrastructure and funded by BEIS capital funding via STFC capital Grants No. ST/P002293/1, No. ST/R002371/1, and No. ST/S002502/1, Durham University and STFC operations Grant No. ST/R000832/1. This work was partly performed in part at Aspen Center for Physics, which National Science Foundation supports Grant No. PHY-2210452.

APPENDIX A: GAUGE UNIFICATION

A necessary condition for a realistic GUT model is that all gauge couplings unified to a single gauge coupling at a certain scale given by g_{GUT} and M_{GUT}, respectively, up to matching conditions. We begin with the two-loop RGEs. Given an interval of energy scale $Q\in(Q_0,Q_1)$, where the gauge symmetry is $G=H_1\times H_2\times\cdots\times H_n$ and no particles decouple in this period, the coupling $\alpha_i=g_i^2/(4\pi)$ for each gauge symmetry H_i (for $i\in[1,\ldots,n]$) is described by the following differential equation

$$Q\frac{d\alpha_i}{dQ}=\beta_i(\alpha_i). \tag{A1}$$

The β function, up to the two-loop level, is given by

$$\beta_i=-\frac{1}{2\pi}\alpha_i^2\left(b_i+\frac{1}{4\pi}\sum_j b_{ij}\alpha_j\right), \tag{A2}$$

where $i\in[1,\ldots,n]$ for H_n, g_i is the gauge coefficient of H_i, and b_i and b_{ij} refer to the normalized coefficients of one- and two-loop contributions, respectively. In the following, we neglect the Yukawa contribution to the renormalization group (R.G.) running equations as it gives a subdominant contribution. If the conditions $b_j\alpha_j(Q_0)\log(Q/Q_0)<1$ is satisfied, then an analytical solution for these equations can be obtained [78]:

$$\alpha_i^{-1}(Q)=\alpha_i^{-1}(Q_0)-\frac{b_i}{2\pi}\log\frac{Q}{Q_0}+\sum_j\frac{b_{ij}}{4\pi b_i}\log\left(1-\frac{b_j}{2\pi}\alpha_j(Q_0)\log\frac{Q}{Q_0}\right). \tag{A3}$$

TABLE II. Coefficients b_i and b_{ij} of gauge coupling β functions appearing in the specified breaking chain. In this table, we identify the scale of gauge symmetry as the corresponding heavy gauge boson mass from the effective field theory (EFT) point of view. The SUSY breaking scale $M_{\rm MSSM}$ is regarded as the unified mass of all sfermions. In the split SUSY, gauge bosons and Higgs superpartners are allowed to be different from and usually a few orders of magnitude lower than the SUSY-breaking scale. We also consider the possibility of having a further gap between the wino and gluino masses and the bino and Higgsino masses. We include their threshold effect in the RG running.

SO(10)	Broken at $Q = M_{\rm GUT}$
↓	$\{b_i\} = \begin{pmatrix} -3 \\ 2 \\ -1 \\ \frac{21}{2} \end{pmatrix}$, $\{b_{ij}\} = \begin{pmatrix} 14 & 9 & 9 & 1 \\ 24 & 32 & 6 & 3 \\ 24 & 6 & 56 & 15 \\ 8 & 9 & 45 & 34 \end{pmatrix}$
$G_{\rm int}$	Broken at $Q = M_{B-L}$
↓	$\{b_i\} = \begin{pmatrix} -3 \\ 1 \\ \frac{33}{5} \end{pmatrix}$, $\{b_{ij}\} = \begin{pmatrix} 14 & 9 & \frac{11}{5} \\ 24 & 25 & \frac{9}{5} \\ \frac{88}{5} & \frac{27}{5} & \frac{199}{25} \end{pmatrix}$
$G_{\rm MSSM}$	Broken at $Q = M_{\rm MSSM}$
↓	$\{b_i\} = \begin{pmatrix} -5 \\ -\frac{7}{6} \\ \frac{9}{2} \end{pmatrix}$, $\{b_{ij}\} = \begin{pmatrix} 22 & \frac{9}{2} & \frac{11}{10} \\ 12 & \frac{106}{3} & \frac{6}{5} \\ \frac{44}{5} & \frac{18}{5} & \frac{104}{25} \end{pmatrix}$
Wino and gluino decoupling	Happening at $Q = M_{\tilde{W}}$
↓	$\{b_i\} = \begin{pmatrix} -7 \\ -\frac{5}{2} \\ \frac{9}{2} \end{pmatrix}$, $\{b_{ij}\} = \begin{pmatrix} -26 & \frac{9}{2} & \frac{11}{10} \\ 12 & 14 & \frac{6}{5} \\ \frac{44}{5} & \frac{18}{5} & \frac{104}{25} \end{pmatrix}$
Bino and Higgsino decoupling	Happening at $Q = M_{\tilde{B}}$
↓	$\{b_i\} = \begin{pmatrix} -7 \\ -\frac{19}{6} \\ \frac{41}{10} \end{pmatrix}$, $\{b_{ij}\} = \begin{pmatrix} -26 & \frac{9}{2} & \frac{11}{10} \\ 12 & \frac{35}{6} & \frac{9}{10} \\ \frac{44}{5} & \frac{17}{10} & \frac{199}{50} \end{pmatrix}$
$G_{\rm SM}$	

In non-SUSY and SUSY, the coefficients b_i and b_{ij} are, respectively, given by

$$\text{non-SUSY:}\ b_i = -\frac{11}{3}C_2(H_i) + \frac{2}{3}\sum_{\psi} T(\psi_i) + \frac{1}{3}\sum_{\phi} T(\phi_i),$$
$$b_{ij} = -\frac{34}{3}[C_2(H_i)]^2\delta_{ij} + \sum_{\psi} T(\psi_i)\left[2C_2(\psi_j) + \frac{10}{3}C_2(H_i)\delta_{ij}\right] + \sum_{\phi} T(\phi_i)\left[4C_2(\phi_j) + \frac{2}{3}C_2(H_i)\delta_{ij}\right]; \quad \text{(A4)}$$

$$\text{SUSY:}\ b_i = -3C_2(H_i) + \sum_{\tilde{\Phi}} T(\tilde{\Phi}_i),$$
$$b_{ij} = -6[C_2(H_i)]^2\delta_{ij} + \sum_{\tilde{\Phi}} 2T(\tilde{\Phi}_i)[C_2(H_i)\delta_{ij} + 2C_2(\tilde{\Phi}_j)], \quad \text{(A5)}$$

where ϕ, ψ, and $\tilde{\Phi}$ represent any complex scalar, chiral fermion and chiral superfield evolving in the scale between Q_0 and Q_1, respectively, $C_2(H_i)$ is the quadratic Casimir invariant of the adjoint presentation in the group H_i, $C_2(\phi_i)$ ($C_2(\tilde{\Phi}_i)$) is quadratic Casimir invariant of the representation of the field ϕ (superfield $\tilde{\Phi}$) in the group H_i, $T(\phi_i)$ ($T(\tilde{\Phi}_i)$) is the Dynkin index of the field ϕ (superfield $\tilde{\Phi}$) in group H_i, and the summation goes over all fields (superfields). In our model, values of coefficients b_i and b_{ij} in each interval of the energy scale from $M_{\rm GUT}$ down to M_Z are shown in Table II.

At the intermediate scale, where a larger symmetry is broken to its subsymmetry, gauge couplings between them satisfy matching conditions. Here we list one-loop

matching conditions that appear in the GUT-breaking chains. For a simple Lie group H_{i+1} broken to subgroup H_i at the scale $Q = M_I$, the one-loop matching condition in the $\overline{\text{MS}}$ scheme is given by [79]

$$H_{i+1} \to H_i:$$
$$\alpha^{-1}_{H_{i+1}}(M_I) - \frac{1}{12\pi} C_2(H_{i+1}) = \alpha^{-1}_{H_i}(M_I) - \frac{1}{12\pi} C_2(H_i). \quad \text{(A6)}$$

Above the SUSY scale, the couplings must run in the $\overline{\text{D.R.}}$ scheme to preserve the supersymmetry [80]. The relation of couplings in the $\overline{\text{MS}}$ scheme and $\overline{\text{DR}}$ scheme is described by

$$\alpha^{-1}_{\text{DR}} = \alpha^{-1}_{\text{MS}} - \frac{1}{12\pi} C_2(H_i). \quad \text{(A7)}$$

Thus the one-loop matching condition in the $\overline{\text{DR}}$ scheme is simply

$$H_{i+1} \to H_i:\ \alpha^{-1}_{H_{i+1}}(M_I) = \alpha^{-1}_{H_i}(M_I). \quad \text{(A8)}$$

For $G_{\text{int}} \to G_{\text{MSSM}}$, we encounter the breaking, $SU(2)_R \times U(1)_X \to U(1)_Y$, where $U(1)_X$ is identical to $U(1)_{B-L}$ with the charge normalized as $X = \sqrt{3/8}(B-L)$. The matching condition in $\overline{\text{DR}}$ scheme is given by

$$SU(2)_R \times U(1)_X \to U(1)_Y:$$
$$\frac{3}{5}\alpha^{-1}_{2R}(M_{B-L}) + \frac{2}{5}\alpha^{-1}_{1X}(M_{B-L}) = \alpha^{-1}_{1Y}(M_{B-L}). \quad \text{(A9)}$$

Applying the matching conditions, all gauge couplings of the subgroups unify into a single gauge coupling of SO(10) at the GUT scale, M_{GUT}. This condition restricts both the GUT and intermediate scales for each breaking chain. We denote the mass of the heavy gauge boson masses associated with SO(10) breaking as M_{GUT} while M_{B-L} and M_{SUSY} are associated to the breaking of G_{int} and G_{MSSM}, respectively.

TABLE III. Decomposition of the Higgses which induce spontaneous symmetry breaking at each step of the breaking chain. Each Higgs (from left to right) is eventually decomposed to a singlet whose nonvanishing VEV preserves the symmetry G_I (for $I = 3, 2, 1, \text{SM}$) in the same row but breaks larger symmetries. The subscript S refers to $\overline{\mathbf{126}}$ containing a SM singlet scalar whose VEV generates the RHN masses via B-L symmetry breaking.

SO(10)	45	$\overline{126}$
G_{int}	$(\mathbf{1},\mathbf{1},\mathbf{1},0)$	$(\mathbf{1},\mathbf{1},\mathbf{3},-1)$
G_{SM}	$(\mathbf{1},\mathbf{1},0)$	$(\mathbf{1},\mathbf{1},0)_S$

APPENDIX B: MATTER AND HIGGS DECOMPOSITION

The **45** and $\overline{\mathbf{126}}$ are required for gauge symmetry breaking, and we list their decomposition under $G_{\text{int}} \equiv SU(3)_c \times SU(2)_L \times SU(2)_R \times U(1)_{B-L} \times \text{SUSY}$ and $G_{\text{SM}} \equiv SU(3)_c \times SU(2)_L \times U(1)_Y$ in Table III.

We include two further Higgs multiplets, **10** and **120**, to generate the Standard Model fermion masses [81]. We show their decompositions under G_1 and G_{SM} in Table IV where the subscript is used to distinguish fields with the same representation. In Table IV, $\overline{\mathbf{126}}$ is the same Higgs used in the breaking $G_{\text{int}} \to G_{\text{SM}}$ that has the dual role of spontaneous symmetry breaking and flavor structure generation.

The fermions are arranged as a **16** of SO(10) and follow the decomposition given in Table V where L (R) denote the left-handed (right-handed) fermions of G_3 which contains the SM left-handed (right-handed) fermions where $Q_{L(R)}$ and $\ell_{L(R)}$ are the quark and leptonic $SU(2)_{L(R)}$ doublets, respectively, and u_R, d_R, e_R, and ν_R are the quark and lepton $SU(2)_L$ singlets, respectively.

APPENDIX C: CORRELATIONS OF FERMION MASSES AND MIXING

In this section, we present the correlations of masses and mixing between quarks and leptons and predict the RHN masses using the model we discussed in the previous

TABLE IV. Decomposition of Higgses responsible for the fermion mass generation. $\overline{\mathbf{126}}$ is the same Higgs as shown in Table III and it is responsible for both the breaking $G_{\text{int}} \to G_{\text{SM}}$ and right-handed neutrino mass generation. $(\mathbf{1},\mathbf{1},0)_S$ is the same singlet given in Table III.

SO(10)	10	$\overline{126}$	120
G_{int}	$(\mathbf{1},\mathbf{2},\mathbf{2},0)_1$	$(\mathbf{1},\mathbf{2},\mathbf{2},0)_2$ $+(\mathbf{1},\mathbf{1},\mathbf{3},-1)$	$(\mathbf{1},\mathbf{2},\mathbf{2},0)_{3,4}$
G_{SM}	$(\mathbf{1},\mathbf{2},-1/2)_{h^u_{\mathbf{10}}}$ $+(\mathbf{1},\mathbf{2},+1/2)_{h^d_{\mathbf{10}}}$	$(\mathbf{1},\mathbf{2},-1/2)_{h^u_{\overline{\mathbf{126}}}}$ $+(\mathbf{1},\mathbf{2},+1/2)_{h^d_{\overline{\mathbf{126}}}}$ $+(\mathbf{1},\mathbf{1},0)_S$	$(\mathbf{1},\mathbf{2},-1/2)_{h^u_{\mathbf{120}},h^{u'}_{\mathbf{120}}}$ $+(\mathbf{1},\mathbf{2},+1/2)_{h^d_{\mathbf{120}},h^{d'}_{\mathbf{120}}}$

TABLE V. Decomposition of the matter multiplet **16** in each step of the breaking chain.

SO(10)	16
$G_{\rm int}$	$(\mathbf{3},\mathbf{2},\mathbf{1},1/6)_{Q_L}+(\bar{\mathbf{3}},\mathbf{1},\mathbf{2},-1/6)_{Q_R^c}$ $+(\mathbf{1},\mathbf{2},\mathbf{1},-1/2)_{l_L}+(\mathbf{1},\mathbf{1},\mathbf{2},1/2)_{l_R^c}$
$G_{\rm SM}$	$(\mathbf{3},\mathbf{2},1/6)_{Q_L}+(\bar{\mathbf{3}},\mathbf{1},-2/3)_{u_R^c}+(\bar{\mathbf{3}},\mathbf{1},1/3)_{d_R^c}$ $+(\mathbf{1},\mathbf{2},-1/2)_{l_L}+(\mathbf{1},\mathbf{1},0)_{\nu_R^c}+(\mathbf{1},\mathbf{1},1)_{e_R^c}$

section. We parametrize the up, down, neutrino, charged lepton Yukawa couplings and right-handed neutrino mass matrix following the left-right notation in Refs. [83–86], respectively, as follows:

$$\begin{aligned} Y_u &= h + r_2 f + i r_3 h', \qquad Y_d = r_1(h + f + i h'),\\ Y_\nu &= h - 3 r_2 f + i c_\nu h', \qquad Y_e = r_1(h - 3f + i c_e h'),\\ M_{\nu_R} &= f\frac{\sqrt{3} r_1}{U_{12}} v_S, \end{aligned} \tag{C1}$$

where

$$\begin{aligned} h &= Y_{\mathbf{10}} V_{11}, \quad f = Y_{\overline{\mathbf{126}}}\frac{U_{12}}{\sqrt{3}}\frac{V_{11}}{U_{11}},\\ h' &= -iY_{\mathbf{120}}(U_{13} + U_{14}/\sqrt{3})\frac{V_{11}}{U_{11}},\\ r_1 &= \frac{U_{11}}{V_{11}}, \quad r_2 = \frac{V_{12}}{U_{12}}\frac{U_{11}}{V_{11}}, \quad r_3 = \frac{V_{13} + V_{14}/\sqrt{3}}{U_{13} + U_{14}/\sqrt{3}}\frac{U_{11}}{V_{11}},\\ c_e &= \frac{U_{13} - \sqrt{3} U_{14}}{U_{13} + U_{14}/\sqrt{3}}, \quad c_\nu = \frac{V_{13} - \sqrt{3} V_{14}}{U_{13} + U_{14}/\sqrt{3}}\frac{U_{11}}{V_{11}}, \end{aligned} \tag{C2}$$

and V_{ij} and U_{ij} denotes the mixing between the mass and interaction basis of Higgs doublets in the up and down sectors, respectively, before the SUSY breaking [84,85], and v_S is the vacuum expectation value (VEV) of singlet component of $\overline{\mathbf{126}}$ that gives mass to the RHNs. The light neutrino mass matrix, M_ν, is obtained by

$$M_\nu = m_0 Y_\nu f^{-1} Y_\nu, \tag{C3}$$

where $m_0 = -\frac{U_{12}}{\sqrt{3} r_1}\frac{v_u^2}{v_S}$. Once the scale v_S is determined, U_{12} can be solved as

$$U_{12} = -\sqrt{3} r_1 \frac{m_0 v_S}{v_u^2}. \tag{C4}$$

The most general form of Yukawa couplings and neutrino mass matrix includes many free parameters. A considerable reduction in the number of parameters can be achieved by considering only the Hermitian case for all fermion Yukawa couplings matrices Y_u, Y_d, Y_ν, and Y_e (and M_R should be real as a consequence of the Majorana nature for right-handed neutrinos). Such a reduction can result from spontaneous CP violation [87,88], which assumes that there exists a CP symmetry above the GUT scale, leading to real-valued $Y_{\mathbf{10}}$, $Y_{\overline{\mathbf{126}}}$ and $Y_{\mathbf{120}}$, and the CP is broken by some complex VEVs of Higgs multiplets during GUT or intermediate symmetry breaking. As a result, h, f and h', as well as all parameters on the right-hand side of Eq. (C1), are real. Since h' is antisymmetric, we arrive at Hermitian Dirac Yukawa coupling matrices Y_u, Y_d, Y_ν, and Y_e. The Higgs mixing elements V_{13}, V_{14} and U_{13}, U_{14} are also purely imaginary with the relations

$$\frac{V_{13}}{V_{14}} = \frac{c_\nu/r_3 + 3}{\sqrt{3}(c_\nu/r_3 - 1)}, \qquad \frac{U_{13}}{U_{14}} = \frac{c_e + 3}{\sqrt{3}(c_e - 1)}. \tag{C5}$$

This texture has been widely applied in the literature, e.g., Refs. [84,89,90]. The resulting fermion mass matrices conserve parity symmetry $L \leftrightarrow R$ [88] and following from the assumption that there is no CP violation in the Higgs sector, apart from that of **120**, r_1, r_2, r_3, c_e, and c_ν are all real parameters resulting in a real symmetric right-handed neutrino mass matrix, M_{ν_R}. The CP symmetry in the Yukawa coupling is spontaneously broken after the Higgses gain VEVs.

1. Procedure to fit the quark and lepton flavor data

For simplicity, we assume that $r_3 = 0$, which implies that the imaginary part of Y_u vanishes. As a result, the relation between V_{13} and V_{14} in (C5) is no longer valid. Instead, there is a simpler relation that reads $V_{14} = -\sqrt{3} V_{13}$. It is convenient to write the up-type Yukawa in the diagonal basis

$$Y_u = h + r_2 f = \mathrm{diag}\{\eta_u y_u, \eta_c y_c, \eta_t y_t\}, \tag{C6}$$

which can be achieved via a real-orthogonal transformation on the fermion flavors without changing the Hermitian property of Y_d, Y_e, and Y_ν. In the above, $\eta_{u,c,t} = \pm 1$ refer to signs that the real-orthogonal transformation cannot determine. While $\eta_t = +1$ can be fixed by making an overall sign rotation for all Yukawa matrices, the remaining signs, η_u and η_c, cannot be fixed and are randomly varied throughout our analysis. In the basis of the diagonal up-quark mass matrix, Y_d is given by

$$Y_d = P_a V_{\rm CKM} \mathrm{diag}\{\eta_d y_d, \eta_s y_s, \eta_b y_b\} V_{\rm CKM}^\dagger P_a^*, \tag{C7}$$

where again $\eta_{d,s,b} = \pm 1$ represent the signs of eigenvalues, and $V_{\rm CKM}$ is the CKM matrix parametrized in the following form

$$V_{\rm CKM} = \begin{pmatrix} c_{12}c_{13} & s_{12}c_{13} & s_{13}e^{-i\delta_q} \\ -s_{12}c_{23} - c_{12}s_{13}s_{23}e^{i\delta_q} & c_{12}c_{23} - s_{12}s_{13}s_{23}e^{i\delta_q} & c_{13}s_{23} \\ s_{12}s_{23} - c_{12}s_{13}c_{23}e^{i\delta_q} & -c_{12}s_{23} - s_{12}s_{13}c_{23}e^{i\delta_q} & c_{13}c_{23} \end{pmatrix}, \tag{C8}$$

where $s_{ij}=\sin\theta_{ij}^q$, $c_{ij}=\cos\theta_{ij}^q$, and $P_a=\mathrm{diag}\{e^{ia_1},e^{ia_2},1\}$. The matrices h, f, and h' are then expressed in terms of Y_u and Y_d

$$h = -\frac{Y_u}{r_2-1} + \frac{r_2 \mathrm{Re}Y_d}{r_1(r_2-1)}, \qquad f = \frac{Y_u}{r_2-1} - \frac{\mathrm{Re}Y_d}{r_1(r_2-1)}, \qquad h' = i\frac{\mathrm{Im}Y_d}{r_1}, \tag{C9}$$

where Y_ν, Y_e are

$$Y_\nu = -\frac{3r_2+1}{r_2-1}Y_u + \frac{4r_2}{r_1(r_2-1)}\mathrm{Re}Y_d + i\frac{c_\nu}{r_1}\mathrm{Im}Y_d,$$
$$Y_e = -\frac{4r_1}{r_2-1}Y_u + \frac{r_2+3}{r_2-1}\mathrm{Re}Y_d + ic_e\mathrm{Im}Y_d. \tag{C10}$$

The light neutrino mass matrix can be expressed as

$$M_\nu = m_0\left(\frac{8r_2(r_2+1)}{r_2-1}Y_u - \frac{16r_2^2}{r_1(r_2-1)}\mathrm{Re}Y_d + \frac{r_2-1}{r_1}(r_1Y_u + ic_\nu\mathrm{Im}Y_d)(r_1Y_u - \mathrm{Re}Y_d)^{-1} \times (r_1Y_u - ic_\nu\mathrm{Im}Y_d)\right). \tag{C11}$$

Using this parametrization, all six quark masses and four CKM mixing parameters are treated as inputs, and we are then left with seven parameters (a_1, a_2, r_1, r_2, c_e, c_ν, and m_0) to fit eight observables, including three Yukawa couplings y_e, y_μ, y_τ, two neutrino mass-squared differences Δm_{21}^2, Δm_{31}^2 and three mixing angles θ_{12}, θ_{13}, θ_{23}, where the leptonic CP-violating phase, δ, will be treated as a prediction.

By fitting the fermion mass and mixing, the matrices h, f, h' and parameters a_1, a_2, r_1, r_2, c_e, c_ν, and m_0 can be fully determined. To perform the parameter scan, and find viable regions of the model parameter space that postdict the quark and predict the leptonic data, we run all the SM Yukawa couplings to the GUT scale (using two-loop RGEs, appropriate matching between scales and threshold corrections) using REAP [91,92] and SARAH [93]. We then scan the free parameters of the GUT model as described above and assess how well they fit the leptonic data using the statistical measure below:

$$\chi^2 = \sum_n \left[\frac{\mathcal{O}_n(\mathcal{P}_m) - \mathcal{O}_n^{\rm bf}}{\sigma_{\mathcal{O}_n}}\right]^2, \tag{C12}$$

where $\mathcal{P}_m \in \{a_1,a_2,r_1,r_2,c_e,c_\nu,m_0,\eta_q\}$ and $\mathcal{O}_n \in \{m_e,m_\mu, m_\tau,\theta_{12},\theta_{13},\theta_{23},\Delta m_{21}^2,\Delta m_{31}^2\}$.

Then Yukawa couplings for SO(10) **16** multiplets can be expressed as

$$Y_{\mathbf{10}} = \frac{h}{V_{11}}, \quad Y_{\overline{\mathbf{126}}} = -f\frac{v_u^2}{m_0 v_S}, \quad Y_{\mathbf{120}} = ih'\frac{c_\nu}{4V_{13}}, \tag{C13}$$

this will be relevant for the subsequent discussion on proton decay, tightly linked with the scan of fermion masses and mixing since it is mediated by the Higgs color triplet and the operators computed from the same superpotential. Apart from the matrices and parameters that can be fixed by fermion mass and mixing, there are three parameters: two Higgs mixing elements V_{11} and V_{13} and $\tan\beta$. Apart from the equations above, there are also

$$U_{11} = r_1V_{11}, \quad V_{12} = \frac{r_2}{r_1}U_{12}, \quad U_{13} = \frac{2r_1}{c_\nu}\frac{c_e+3}{c_e+1}V_{13},$$
$$U_{14} = \frac{2\sqrt{3}r_1}{c_\nu}\frac{c_e-1}{c_e+1}V_{13}, \quad V_{14} = -\sqrt{3}V_{13}, \tag{C14}$$

while U_{12} can be solved using (C4). Each element in the mixing matrices has to satisfy the unitarity. We show a subset of our predictions from the scan in Fig. 6. In the left (right) panel, we show the predictions for the muon (δ phase) Yukawa versus the electron Yukawa (θ_{23}). We note that the predictions are consistent with the experimental values at the 3σ level. While all values of δ can be accommodated, the model prefers the atmospheric mixing angle to be in the lower octant. Moreover, the model strongly prefers normally ordered light neutrino masses.

2. A benchmark study

We considered a benchmark point of our scan (yellow star), achieving successful leptogenesis, giving $\eta_B \sim 6.16\times10^{-10}$. Inputs and predictions of fermion Yukawas and mixing parameters are shown in Table VI. From this, the Yukawa and neutrino mass matrices are obtained:

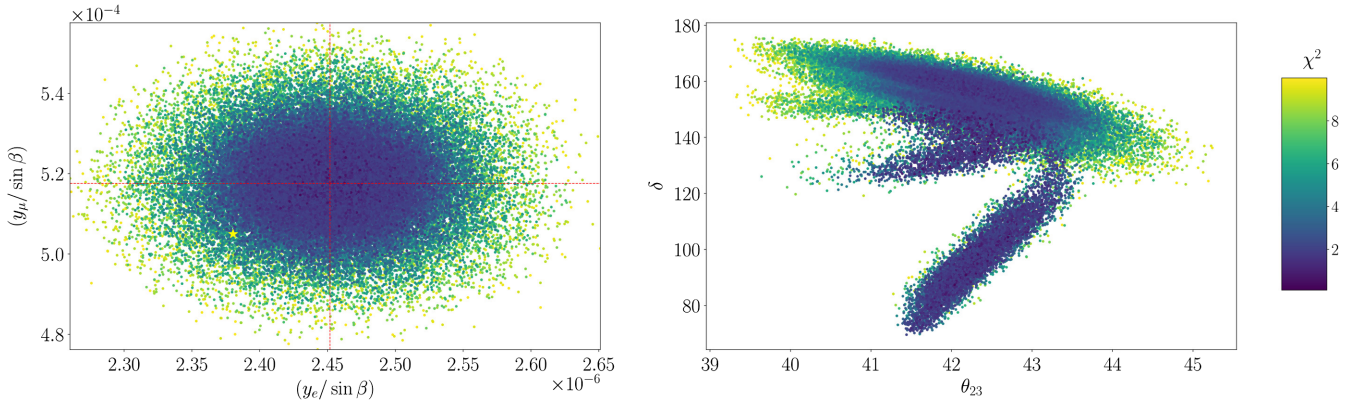

FIG. 6. All colored points show regions of the parameter space that fit the lepton sector with $\chi^2 < 10$. The yellow star shows a benchmark point in the scan with $\eta_B \sim 6.16 \times 10^{-10}$. All the points in the scan predict $-11 \lesssim \log_{10}(\eta_B) \lesssim -8$.

$$Y_u/\cos\beta = \begin{pmatrix} 3.04 \times 10^{-6} & 0 & 0 \\ 0 & 0.00149 & 0 \\ 0 & 0 & 0.489 \end{pmatrix}, \tag{C15}$$

$$Y_d/\sin\beta = 10^{-2} \cdot \begin{pmatrix} -0.0051423 & -0.0039347 + 0.00050024i & 0.0019310 - 0.0013028i \\ -0.0039347 - 0.00050024i & 0.12261 & -0.19878 - 0.17455i \\ 0.0019310 + 0.0013028i & -0.19878 + 0.17455i & 0.61483 \end{pmatrix}, \tag{C16}$$

$$Y_e/\sin\beta = 10^{-2} \cdot \begin{pmatrix} -0.0011843 & -0.00090268i + 0.0064489i & 0.00044301 - 0.016795i \\ -0.00090268i - 0.0064489i & 0.0050731 & -0.0045604 - 0.22502i \\ 0.00044301i + 0.016795i & -0.0045604 + 0.22502i & 0.88287 \end{pmatrix}, \tag{C17}$$

$$M_\nu = \cdot \begin{pmatrix} 6.259 + 6.680i & 4.786 + 2.162i & -2.167 + 1.916i \\ 4.786 + 2.162i & -13.836 + 0.1096i & 26.166 + 8.005i \\ -2.167 + 1.916i & 26.166 + 8.005i & -15.644 - 25.224i \end{pmatrix} \text{meV}. \tag{C18}$$

Diagonalization of Y_e and M_ν gives rise to the lepton masses and mixing, and the above benchmark provides $\chi^2 = 8.22$.

TABLE VI. Inputs and predictions of neutrino masses and the benchmark point mixing parameters fully satisfy all experimental data. Charged fermion masses and CKM mixing are all fixed at experimental best-fit values. Neutrino masses with normal ordering are predicted.

Inputs	a_1 $35, 40°$	a_2 $221.27°$	c_ν -1.49	m_0 44.24 meV	$(\eta_u, \eta_c, \eta_t; \eta_d, \eta_s, \eta_b)$ $(-,+,+;+,-,-)$
Outputs	θ_{13} $8.66°$	θ_{12} $33.19°$	θ_{23} $44.14°$	δ $131.57°$	m_1 5.29 meV
($\chi^2 = 8.22$)	$m_{\beta\beta}$ 5.76 meV		M_{N_1} 8.18×10^{11} GeV	M_{N_2} 1.53×10^{12} GeV	M_{N_3} 4.67×10^{13} GeV

APPENDIX D: PROTON DECAY

Unified theories may contain gauge or scalar bosons that mediate baryon (B) number and lepton number (L) violating processes and hence can cause the decay of nucleons. The dominant mediator is the heavy color gauge boson which leads to proton decay where the most constrained channel is $p \to \pi^0 e^+$ with the lifetime $\tau_{\pi^0 e^+} \gtrsim 2.4 \times 10^{34}$ years set by Super-K [94]. Due to the direct correlation $\tau_{\pi^0 e^+} \propto M_{\rm GUT}^4$, this channel usually provides the most constraining limit on the GUT scale, $M_{\rm GUT} \gtrsim 3 \times 10^{15}$ GeV, almost regardless of the breaking chains of SO(10) [35].

The following section discusses proton decay induced by GUT and SUSY symmetry breaking, respectively.

1. Pion channel

The computation of the proton lifetime in this channel is identical in both the SUSY and the non-SUSY case, and it is carried by the heavy SO(10) gauge bosons. The relevant dimension-six operators are written as

$$\frac{\epsilon_{\alpha\beta}}{\Lambda^2}[(\overline{u_R^c}\gamma^\mu Q_\alpha)(\overline{d_R^c}\gamma_\mu L_\beta) + (\overline{u_R^c}\gamma^\mu Q_\alpha)(\overline{e_R^c}\gamma_\mu Q_\beta) + (\overline{d_R^c}\gamma^\mu Q_\alpha)(\overline{u_R^c}\gamma_\mu L_\beta) + (\overline{d_R^c}\gamma^\mu Q_\alpha)(\overline{\nu_R^c}\gamma_\mu Q_\beta)], \quad \text{(D1)}$$

where color and flavor indices have been suppressed and $\Lambda \simeq \sqrt{2} M_{\rm GUT}/g_{\rm GUT}$ denotes the UV completion scale. The proton lifetime is [35]

$$\Gamma(p \to \pi^0 + e^+) = \frac{m_p}{32\pi}\left(1 - \frac{m_{\pi^0}^2}{m_p^2}\right)^2 A_L^2 [A_{SL}\Lambda_1^{-2}(1 + |V_{ud}|^2)|\langle \pi^0|(ud)Ru_L|p\rangle|^2 + A_{SR}(\Lambda_1^{-2} + |V_{ud}|^2\Lambda_2^{-2})|\langle \pi^0|(ud)_L u_L|p\rangle|^2], \quad \text{(D2)}$$

The enhancement factors denoted as A_L, $A_{S.L.}$, and $A_{S.R.}$, correspond to the influence of long and short-range effects on proton decay. The relevant hadronic matrix element for this particular decay mode is $\langle \pi^0|(ud)_{L,R}u_L|p\rangle$, which has been determined through a QCD lattice simulation [95]. The long-range effect incorporates the renormalization enhancement from the proton decay process (at scales ~1 GeV) to the electroweak scale (defined as the mass of the Z boson at the scale of M_Z). This enhancement factor, calculated at the two-loop level, for is $A_L = 1.247$ in the studies [96]. In the SUSY case, we used $A_L = 0.4$ [97,98]. The short-range factors are determined through the renormalization group equations, which span from the scale M_Z to $M_{\rm GUT}$:

$$A_{SL(R)} = \prod_{A}^{M_Z \le M_A \le M_{\rm GUT}} \prod_i \left[\frac{\alpha_i(M_{A+1})}{\alpha_i(M_A)}\right]^{\frac{\gamma_{iL(R)}}{b_i}}, \quad \text{(D3)}$$

where γ_i are the anomalous dimensions and b_i the one-loop β coefficients.

2. Kaon channel

For the computation of the proton decay in the kaon channel, we followed the treatment of Refs. [99,100]. The baryon number violating interaction is mediated by the Higgs color triplet with mass $M_T \simeq M_{\rm GUT}$. The terms in the superpotential, which we consider, are the same as the Yukawa sector in Eq. (2). Let us consider the effective superpotential from which we can infer all the five-dimensional operators contributing to the kaon channel,

$$W_{\Delta B=1} = \frac{\epsilon_{abc}}{M_T}(C^L_{\alpha\beta\gamma\delta} Q^a_\alpha Q^b_\beta Q^c_\gamma L_l + C^R_{[\alpha\beta\gamma]\delta} U^{\mathcal{C}a}_\alpha D^{\mathcal{C}b}_\beta U^{\mathcal{C}c}_\gamma E^{\mathcal{C}}_\delta),$$

where the matter should be understood as chiral superfield, a, b, c are colors indices and α, β, γ, δ are flavor indexes and C^L_{ijkl} and C^R_{ijkl} are the Wilson coefficients, and in the flavor basis they are expressed as

$$\begin{aligned} C^R_{\alpha\beta\gamma\delta} &= (Y_{\mathbf{10}})_{\alpha\beta}(Y_{\mathbf{10}})_{\gamma\delta} + x_1(Y_{\overline{\mathbf{126}}})_{\alpha\beta}(Y_{\overline{\mathbf{126}}})_{\gamma\delta} + x_2(Y_{\mathbf{120}})_{\alpha\beta}(Y_{\mathbf{120}})_{\gamma\delta} + x_3(Y_{\mathbf{10}})_{\alpha\beta}(Y_{\overline{\mathbf{126}}})_{\gamma\delta} \\ &+ x_4(Y_{\overline{\mathbf{126}}})_{\alpha\beta}(Y_{\mathbf{10}})_{\gamma\delta} + x_5(Y_{\overline{\mathbf{126}}})_{\alpha\beta}(Y_{\mathbf{120}})_{\gamma\delta} + x_6(Y_{\mathbf{120}})_{\alpha\beta}(Y_{\overline{\mathbf{126}}})_{\gamma\delta} + x_7(Y_{\mathbf{10}})_{\alpha\beta}(Y_{\mathbf{120}})_{\gamma\delta} \\ &+ x_8(Y_{\mathbf{120}})_{\alpha\beta}(Y_{\mathbf{10}})_{\gamma\delta} + x_9(Y_{\overline{\mathbf{126}}})_{\alpha\delta}(Y_{\mathbf{120}})_{\beta\gamma} + x_{10}(Y_{\mathbf{120}})_{\alpha\delta}(Y_{\mathbf{120}})_{\beta\gamma}, \\ C^L_{\alpha\beta\gamma\delta} &= (Y_{\mathbf{10}})_{\alpha\beta}(Y_{\mathbf{10}})_{\gamma\delta} + x_1(Y_{\overline{\mathbf{126}}})_{\alpha\beta}(Y_{\overline{\mathbf{126}}})_{\gamma\delta} - x_3(Y_{\mathbf{10}})_{\alpha\beta}(Y_{\overline{\mathbf{126}}})_{\gamma\delta} - x_4(Y_{\overline{\mathbf{126}}})_{\alpha\beta}(Y_{\mathbf{10}})_{\gamma\delta} \\ &+ y_5(Y_{\overline{\mathbf{126}}})_{\alpha\beta}(Y_{\mathbf{120}})_{\gamma\delta} + y_7(Y_{\mathbf{10}})_{\alpha\beta}(Y_{\mathbf{120}})_{\gamma\delta} + y_9(Y_{\mathbf{120}})_{\alpha\gamma}(Y_{\overline{\mathbf{126}}})_{\beta\delta} + y_{10}(Y_{\mathbf{120}})_{\alpha\gamma}(Y_{\mathbf{120}})_{\beta\delta}, \end{aligned} \quad \text{(D4)}$$

where x_i and y_i are the matrices' elements that diagonalize the color triplet mass matrix and can be treated as free parameters that we vary randomly in the interval [0, 1]. In Eq. (D4) all the Yukawa couplings are rotated to be in the mass basis. The coefficients $C^L_{\alpha\beta\gamma\delta}$ and $C^R_{\alpha\beta\gamma\delta}$ induces uncertainties for the partial lifetime. Fitting of fermion masses and mixing helps to obtain h, g, and h', overall factors between them and $Y_{\mathbf{10}}$, $Y_{\mathbf{126}}$, and $Y_{\mathbf{120}}$, in particular, V_{11} between h and $Y_{\mathbf{10}}$, are undermined. By requiring the perturbativity of the theory, we scan and obtain the maximal and minimal contributions of these coefficients to the proton decay. In Fig. (4), the exclusion region for mass scales set by Super-K and the future sensitivity of JUNO is obtained by considering the maximal and minimal contribution of coefficients, respectively.

In order to be able to predict proton decay, the squarks or the sleptons in the five-dimensional operators of Eq. (D4) need to be dressed with gaugino or Higgsino vertices. We note that from the model's symmetry, namely that a bino or a gluino dressing gives zero contribution due to the Fierz identity, only the contributions from the wino and the Higgsino dressing significantly promote decay in this channel. In contrast, the dressing from gluino and binos is negligible. The suboperators we consider are [99,100]

$$\begin{aligned}
C^{I}_{\tilde{W}} &= \frac{1}{2}(\overline{u^c_L} d_{L\beta}) C^L_{[\alpha\beta 1]\delta} U^d_{\alpha\alpha'} U^{\nu}_{\delta\delta'} (\overline{d^c_{L\alpha'}} \nu_{L\delta'}),\\
C^{IV}_{\tilde{W}} &= -\frac{1}{2}(\overline{d^c_{L\beta}} \nu_{L\delta}) C^L_{\alpha[\beta\gamma]\delta} U^d_{1\alpha'} U^{u}_{\gamma 1} (\overline{d^c_{L\alpha'}} u_L),\\
C^{III}_{\tilde{h}^{\pm}} &= -(\overline{d^c_{L\beta}} \nu_{L\delta}) \hat{C}^L_{\alpha[\beta\gamma]\delta} y^{d\dagger}_{\alpha\alpha'} y^{u\dagger}_{\gamma 1} (\overline{d^c_{R\alpha'}} u_R),\\
C^{IV}_{\tilde{h}^{\pm}} &= (\overline{u^c_R} d_{R\beta}) \hat{C}^R_{[\alpha\beta 1]\delta} y^{u}_{\alpha\alpha'} y^{e}_{\delta'} (\overline{d^c_{L\alpha'}} \nu_{L\delta'}),\\
C^{III}_{\tilde{h}^{0}} &= -(\overline{d^c_{L\beta}} \nu_{L\delta}) \hat{C}^L_{\alpha[\beta\gamma]\delta} y^{d\dagger}_{\alpha\alpha'} y^{u\dagger}_{\gamma 1} (\overline{d^c_{R\alpha'}} u_R),
\end{aligned} \tag{D5}$$

where we followed the notation of [100] and the superscripts label the Feynman diagram, which contributes to the kaon channel, and the subscript label the gaugino, which dresses the Feynman diagram. Considering the above suboperators, we note that they are proportional to the mixing matrices and the Yukawa couplings at low energies. Therefore the proton lifetime is tightly linked to the predictions of the scan, and therefore is possible to test the parameter space of the Yukawa sector of the theory with proton decay experiments. In particular, the free parameters on which the overall lifetime depends are r_1, r_2, a_1, a_2, c_e, c_ν, which are fixed from the scan, x_i, y_i, and the Higgs mixing parameters U_{12}, V_{11}, and U_{13}. We found that by randomly varying x_i and y_i, we only achieve a few percent difference in the lifetime while the influence of the Higgs mixing parameters is much more important. The parameter U_{12} can be fixed since it depends on the known parameters m_0, r_1, and M_{B-L}. The other two parameters are constrained by relations of Eq. (C13), and we are considering the highest allowed value.

We can compute the proton decay width considering two different operators proportional to the sum of the coefficients $\mathcal{C}_{\tilde{W}}$ and $\mathcal{C}_h$, which are called, respectively, $\mathcal{O}_{\tilde{W}}$ and $\mathcal{O}_{\tilde{h}}$. These two operators are expressed as

$$\begin{aligned}
\mathcal{O}_{\tilde{W}} &= \left(\frac{i\alpha_2}{4\pi}\right)\left(\frac{1}{M_T}\right) I(M_{\tilde{W}}, m_{\tilde{q}}) \mathcal{C}^{\mathcal{A}}_{\tilde{W}},\\
\mathcal{O}_{\tilde{h}} &= \left(\frac{i}{16\pi^2}\right)\left(\frac{1}{M_T}\right) I(M_{\tilde{h}}, m_{\tilde{q}}) \mathcal{C}^{\mathcal{A}}_{\tilde{h}},
\end{aligned} \tag{D6}$$

where $M_T \sim M_{\mathrm{GUT}}$ is the mass of the Higgs triplet and $I(a,b)$ is the loop contribute; we have $I(a,b) \simeq a/b^2$ when $a \ll b$. Finally, the proton decay width can be expressed in terms of these two operators as

$$\begin{aligned}
\Gamma(p \to K^+ \nu) = \frac{M_p}{8\pi}\left(1 - \frac{m^2_{K^+}}{M^2_p}\right) &\langle K^+ | (us)_L u_L | p \rangle^2\\
&\times A^2_L A^2_S (|\mathcal{O}_{\tilde{W}}|^2 + |\mathcal{O}_{\tilde{h}}|^2).
\end{aligned} \tag{D7}$$

From Eqs. (D6) and (D7), we can also see that the lifetime is highly dependent on the value of the ratio between the gaugino mass and the SUSY breaking scale and from the SUSY breaking scale itself.

[1] H. Fritzsch and P. Minkowski, Ann. Phys. (N.Y.) **93**, 193 (1975).
[2] H. Georgi, Stud. Nat. Sci. **9**, 329 (1975).
[3] H. Georgi, AIP Conf. Proc. **23**, 575 (1975).
[4] T. W. B. Kibble, G. Lazarides, and Q. Shafi, Phys. Lett. **113B**, 237 (1982).
[5] F. An *et al.* (JUNO Collaboration), J. Phys. G **43**, 030401 (2016).
[6] R. Acciarri *et al.* (DUNE Collaboration), arXiv:1512.06148.
[7] K. Abe *et al.* (Hyper-Kamiokande Collaboration), arXiv:1805.04163.
[8] T. W. B. Kibble, J. Phys. A **9**, 1387 (1976).
[9] W. Buchmüller, V. Domcke, K. Kamada, and K. Schmitz, J. Cosmol. Astropart. Phys. 10 (2013) 003.
[10] J. A. Dror, T. Hiramatsu, K. Kohri, H. Murayama, and G. White, Phys. Rev. Lett. **124**, 041804 (2020).
[11] W. Buchmuller, V. Domcke, H. Murayama, and K. Schmitz, Phys. Lett. B **809**, 135764 (2020).

[12] S. Chigusa, Y. Nakai, and J. Zheng, Phys. Rev. D **104**, 035031 (2021).
[13] S. Saad, J. High Energy Phys. 04 (2023) 058.
[14] G. Agazie *et al.* (NANOGrav Collaboration), Astrophys. J. Lett. **951**, L8 (2023).
[15] A. D. Johnson *et al.* (NANOGrav Collaboration), arXiv:2306.16223.
[16] G. Agazie *et al.* (NANOGrav Collaboration), Astrophys. J. Lett. **952**, L37 (2023).
[17] G. Agazie *et al.* (NANOGrav Collaboration), Astrophys. J. Lett. **951**, L10 (2023).
[18] A. Afzal *et al.* (NANOGrav Collaboration), Astrophys. J. Lett. **951**, L11 (2023).
[19] R. w. Hellings and G. s. Downs, Astrophys. J. Lett. **265**, L39 (1983).
[20] J. Antoniadis *et al.* (EPTA Collaboration), Astron. Astrophys. **678**, A50 (2023).
[21] J. Antoniadis *et al.* (EPTA Collaboration), Astron. Astrophys. **678**, A48 (2023).
[22] J. Antoniadis *et al.* (EPTA Collaboration), Astron. Astrophys. **678**, A49 (2023).
[23] J. Antoniadis *et al.* (EPTA Collaboration), arXiv:2306.16226.
[24] J. Antoniadis *et al.* (EPTA Collaboration), arXiv:2306.16227.
[25] C. Smarra *et al.* (EPTA Collaboration), Phys. Rev. Lett. **131**, 171001 (2023).
[26] A. Zic *et al.*, Pub. Astron. Soc. Aust. **40**, e049 (2023).
[27] D. J. Reardon *et al.*, Astrophys. J. Lett. **951**, L7 (2023).
[28] D. J. Reardon *et al.*, Astrophys. J. Lett. **951**, L6 (2023).
[29] H. Xu *et al.*, Res. Astron. Astrophys. **23**, 075024 (2023).
[30] W. Buchmuller, V. Domcke, and K. Schmitz, J. Cosmol. Astropart. Phys. 11 (2023) 020.
[31] S. Antusch, K. Hinze, S. Saad, and J. Steiner, Phys. Rev. D **108**, 095053 (2023).
[32] E. Madge, E. Morgante, C. Puchades-Ibáñez, N. Ramberg, W. Ratzinger, S. Schenk, and P. Schwaller, J. High Energy Phys. 10 (2023) 171.
[33] J. Ellis, M. Lewicki, C. Lin, and V. Vaskonen, Phys. Rev. D **108**, 103511 (2023).
[34] S. F. King, S. Pascoli, J. Turner, and Y.-L. Zhou, Phys. Rev. Lett. **126**, 021802 (2021).
[35] S. F. King, S. Pascoli, J. Turner, and Y.-L. Zhou, J. High Energy Phys. 10 (2021) 225.
[36] B. Fu, S. F. King, L. Marsili, S. Pascoli, J. Turner, and Y.-L. Zhou, J. High Energy Phys. 11 (2022) 072.
[37] M. Fukugita and T. Yanagida, Phys. Lett. B **174**, 45 (1986).
[38] G. F. Giudice and A. Romanino, Nucl. Phys. **B699**, 65 (2004); **B706**, 487(E) (2005).
[39] N. Arkani-Hamed and S. Dimopoulos, J. High Energy Phys. 06 (2005) 073.
[40] R. L. Workman *et al.* (Particle Data Group Collaboration), Prog. Theor. Exp. Phys. **2022**, 083C01 (2022).
[41] Y. Aoki *et al.* (Flavour Lattice Averaging Group (FLAG) Collaboration), Eur. Phys. J. C **82**, 869 (2022).
[42] F. Feroz, M. P. Hobson, and M. Bridges, Mon. Not. R. Astron. Soc. **398**, 1601 (2009).
[43] A. Granelli, K. Moffat, Y. F. Perez-Gonzalez, H. Schulz, and J. Turner, Comput. Phys. Commun. **262**, 107813 (2021).
[44] A. Granelli, C. Leslie, Y. F. Perez-Gonzalez, H. Schulz, B. Shuve, J. Turner, and R. Walker, Comput. Phys. Commun. **291**, 108834 (2023).
[45] N. Aghanim *et al.* (Planck Collaboration), Astron. Astrophys. **641**, A6 (2020); **652**, C4(E) (2021).
[46] N. Abgrall *et al.* (LEGEND Collaboration), arXiv:2107.11462.
[47] G. Adhikari *et al.* (nEXO Collaboration), J. Phys. G **49**, 015104 (2022).
[48] F. Agostini *et al.* (DARWIN Collaboration), Eur. Phys. J. C **80**, 808 (2020).
[49] S. Andringa *et al.* (SNO+ Collaboration), Adv. High Energy Phys. **2016**, 6194250 (2016).
[50] E. Armengaud *et al.*, Eur. Phys. J. C **80**, 44 (2020).
[51] A. Boyle, J. Cosmol. Astropart. Phys. 04 (2019) 038; 10 (2019) E01.
[52] B. Audren, J. Lesgourgues, S. Bird, M. G. Haehnelt, and M. Viel, J. Cosmol. Astropart. Phys. 01 (2012) 026.
[53] A. Chudaykin and M. M. Ivanov, J. Cosmol. Astropart. Phys. 11 (2019) 034.
[54] A. Abada *et al.* (FCC Collaboration), Eur. Phys. J. C **79**, 474 (2019).
[55] K. Abe *et al.* (Super-Kamiokande Collaboration), Phys. Rev. D **90**, 072005 (2014).
[56] M. Low and L.-T. Wang, J. High Energy Phys. 08 (2014) 161.
[57] H. Fukuda, F. Luo, and S. Shirai, J. High Energy Phys. 04 (2018) 107.
[58] S. Profumo, Phys. Rev. D **72**, 103521 (2005).
[59] T. Cohen, M. Lisanti, A. Pierce, and T. R. Slatyer, J. Cosmol. Astropart. Phys. 10 (2013) 061.
[60] T. Vachaspati and A. Vilenkin, Phys. Rev. D **31**, 3052 (1985).
[61] A. Vilenkin, Phys. Rep. **121**, 263 (1985).
[62] W. Buchmuller, V. Domcke, and K. Schmitz, Phys. Lett. B **811**, 135914 (2020).
[63] M. A. Masoud, M. U. Rehman, and Q. Shafi, J. Cosmol. Astropart. Phys. 11 (2021) 022.
[64] While the factor $f_{\rm m}$ in the monopole mass is assumed to be of order one [101], it is worth noting that $f_{\rm m} \to 0$ could happen in the case of nonmaximal symmetry breaking [102]. In the latter case, $M_{\rm GUT} \gg m_{\rm m} \sim \sqrt{\mu}$ is still allowed. Thus, we should remember that $M_{B-L} \ll M_{\rm GUT}$ could still be achievable when fitting the NANOGrav data for some special SUSY GUT models.
[65] A. Vilenkin, Nucl. Phys. **B196**, 240 (1982).
[66] J. Preskill and A. Vilenkin, Phys. Rev. D **47**, 2324 (1993).
[67] L. Leblond, B. Shlaer, and X. Siemens, Phys. Rev. D **79**, 123519 (2009).
[68] A. Monin and M. B. Voloshin, Phys. Rev. D **78**, 065048 (2008).
[69] W. Buchmuller, V. Domcke, and K. Schmitz, J. Cosmol. Astropart. Phys. 12 (2021) 006.
[70] R. Abbott *et al.* (KAGRA, Virgo, and LIGO Scientific Collaborations), Phys. Rev. D **104**, 022004 (2021).
[71] G. S. F. Guedes, P. P. Avelino, and L. Sousa, Phys. Rev. D **98**, 123505 (2018).
[72] J. Ellis and M. Lewicki, Phys. Rev. Lett. **126**, 041304 (2021).

[73] G. Aad, B. Abbott, and D. C. Abbott, Eur. Phys. J. C **81**, 1118 (2021).
[74] X. Cid Vidal *et al.*, CERN Yellow Rep. Monogr. **7**, 585 (2019).
[75] H. Cheng (CEPC Physics Study Group), *The Physics potential of the CEPC. Prepared for the US Snowmass Community Planning Exercise* (Snowmass, 2021).
[76] G. Altarelli and D. Meloni, J. High Energy Phys. 08 (2013) 021.
[77] www.dirac.ac.uk.
[78] S. Bertolini, L. Di Luzio, and M. Malinsky, Phys. Rev. D **80**, 015013 (2009).
[79] J. Chakrabortty, R. Maji, S. K. Patra, T. Srivastava, and S. Mohanty, Phys. Rev. D **97**, 095010 (2018).
[80] S. P. Martin and M. T. Vaughn, Phys. Lett. B **318**, 331 (1993).
[81] It has been argued in Ref. [82] that a **10** and a **126** are enough to reproduce the fermion data.
[82] K. S. Babu, B. Bajc, and S. Saad, J. High Energy Phys. 10 (2018) 135.
[83] G. Altarelli and G. Blankenburg, J. High Energy Phys. 03 (2011) 133.
[84] B. Dutta, Y. Mimura, and R. N. Mohapatra, Phys. Rev. Lett. **94**, 091804 (2005).
[85] B. Dutta, Y. Mimura, and R. N. Mohapatra, Phys. Rev. D **72**, 075009 (2005).
[86] B. Dutta, Y. Mimura, and R. N. Mohapatra, Phys. Rev. D **80**, 095021 (2009).
[87] W. Grimus and H. Kuhbock, Phys. Lett. B **643**, 182 (2006).
[88] W. Grimus and H. Kuhbock, Eur. Phys. J. C **51**, 721 (2007).
[89] B. Dutta, Y. Mimura, and R. N. Mohapatra, Phys. Lett. B **603**, 35 (2004).
[90] A. S. Joshipura and K. M. Patel, Phys. Rev. D **83**, 095002 (2011).
[91] S. Antusch, J. Kersten, M. Lindner, M. Ratz, and M. A. Schmidt, J. High Energy Phys. 03 (2005) 024.
[92] S. Antusch and C. Sluka, J. High Energy Phys. 07 (2016) 108.
[93] F. Staub, Adv. High Energy Phys. **2015**, 840780 (2015).
[94] A. Takenaka *et al.* (Super-Kamiokande Collaboration), Phys. Rev. D **102**, 112011 (2020).
[95] Y. Aoki, T. Izubuchi, E. Shintani, and A. Soni, Phys. Rev. D **96**, 014506 (2017).
[96] J. Ellis, M. A. G. Garcia, N. Nagata, D. V. Nanopoulos, and K. A. Olive, J. High Energy Phys. 05 (2020) 021.
[97] J. R. Ellis, D. V. Nanopoulos, and S. Rudaz, Nucl. Phys. **B202**, 43 (1982).
[98] J. Hisano, H. Murayama, and T. Yanagida, Nucl. Phys. **B402**, 46 (1993).
[99] H. S. Goh, R. N. Mohapatra, S. Nasri, and S.-P. Ng, Phys. Lett. B **587**, 105 (2004).
[100] M. Severson, Phys. Rev. D **92**, 095026 (2015).
[101] J. Preskill, Annu. Rev. Nucl. Part. Sci. **34**, 461 (1984).
[102] E. J. Weinberg and P. Yi, Phys. Rep. **438**, 65 (2007).